

MAX PLANCK INSTITUTE FOR INTELLIGENT SYSTEMS

Technical Report No. 3

7 February 2012

HIGH GAMMA-POWER PREDICTS PERFORMANCE IN BRAIN-COMPUTER INTERFACING

Moritz Grosse-Wentrup and Bernhard Schölkopf

Abstract. Subjects operating a brain-computer interface (BCI) based on sensorimotor rhythms exhibit large variations in performance over the course of an experimental session. Here, we show that high-frequency γ -oscillations, originating in fronto-parietal networks, predict such variations on a trial-to-trial basis. We interpret this finding as empirical support for an influence of attentional networks on BCI-performance via modulation of the sensorimotor rhythm.

High Gamma-Power Predicts Performance in Brain-Computer Interfacing

Moritz Grosse-Wentrup & Bernhard Schölkopf

Max Planck Institute for Intelligent Systems, Department Empirical Inference,
Spemannstr. 38, 72076 Tübingen, Germany

E-mail: moritzgw@ieee.org, bs@tuebingen.mpg.de

Abstract. Subjects operating a brain-computer interface (BCI) based on sensorimotor rhythms exhibit large variations in performance over the course of an experimental session. Here, we show that high-frequency γ -oscillations, originating in fronto-parietal networks, predict such variations on a trial-to-trial basis. We interpret this finding as empirical support for an influence of attentional networks on BCI-performance via modulation of the sensorimotor rhythm.

1. Introduction

Subjects operating a non-invasive brain-computer interface (BCI) exhibit large variations in performance over the course of an experimental session. Consider Figure 1, displaying trial-to-trial variations in performance of one representative subject using a two-class motor-imagery BCI. Here, each cross represents one out of 120 trials, recorded over the course of 20 minutes. The y-axis represents the certainty of the employed machine-learning algorithm in decoding the subject’s intention, with the green and red regions indicating correctly and incorrectly classified trials, respectively (the details of the experimental paradigm and decoding procedure are described in Section 2). In the first minutes of the session, the subject was capable of communicating his intention to the BCI with perfect accuracy, with no trials falling into the red region. Several minutes into the session performance started to decline and reached chance-level after around 13 minutes. The subject’s performance started to recover only towards the end of the experiment. Such a temporal structure is quite typical for within-session variations in BCI-performance. As the decoding algorithm of a BCI is usually held fixed throughout a session (cf. [1–3] for notable exceptions), an explanation for these variations has to be found in the subjects’ brain states. The present article aims to identify (some of) the responsible brain processes.

Performance variations in brain-computer interfacing may be studied on several levels, ranging from anatomical [4] to psychological factors [5–8]. The focus of the present study on the neurophysiological level is motivated by the following considerations. Suppose that recordings from brain area A are used for decoding a subject’s intention. Further, assume that there exists a brain region B that does not provide any information on the subject’s goals, yet affects decoding performance by modulating neural activity in A . For example, it is conceivable that the neural substrate of attention modulates the strength of the sensorimotor-rhythm (SMR), thereby affecting performance in motor-imagery BCIs. There are at least four strategies by which such knowledge might be utilized. First, the initiation of a new trial could be delayed until a state of B is observed that is likely to result in a successful inference of the subject’s intention. Second, neurofeedback on activity levels of B might be used to teach subjects how to acquire and maintain a state-of-mind beneficial for operating a BCI. Third, area B could be stimulated, e.g., by transcranial direct current stimulation (TDCS), in order to induce the desired state-of-mind. And fourth, activity levels in B could be used to adapt the decoding algorithm to potential non-stationarities that B might induce in the feature space recorded from A .

Recently, Blankertz et al. demonstrated that the resting-state amplitude of the SMR, i.e., oscillations in the μ - (9-14 Hz) and β -range (20-30 Hz) over sensorimotor areas, predicts subsequent performance in a motor-imagery BCI [9]. This important insight might be used to enhance BCI-performance by adopting the first two strategies discussed above, i.e., either by delaying the initiation of a new trial until a subject displays a strong SMR or by training the subject to generate a strong resting-state SMR.

It is not suited, however, for the remaining two strategies. These require brain processes that are related to BCI-performance yet do not overlap with those processes used for decoding. In recent work, we have presented empirical evidence for such processes [10]. We could demonstrate that spatially distributed oscillations in the high γ -range (55-85 Hz) are correlated with the extent of SMR-modulation induced by motor-imagery, yet do not provide information on the type of motor-imagery performed by a subject. This led us to hypothesize that they are generated by attentional processes that modulate sensorimotor areas.

In the present article, we extend this line of work. We present empirical evidence that oscillations in the high γ -range are not only correlated with BCI-performance, but can further be used to predict performance on a trial-to-trial basis. We investigate the cortical origins of these oscillations and quantify their relevance for research on BCIs in terms of classification accuracy. We argue that our results provide evidence for an influence of attentional networks on BCI-performance via modulation of the sensorimotor μ -rhythm and suggest novel strategies to reduce variations in BCI-performance. A preliminary version of this work has been published in [11].

2. Methods

2.1. Experimental paradigm

Subjects were placed in a comfortable chair approximately 1.5 m in front of a computer screen and were instructed to perform motor imagery of either the left or the right hand as indicated on the screen. Each trial started with a black screen and a centrally displayed gray fixation cross, subsequently denoted as the baseline period, during which subjects were told to sit quietly and relax. After a randomly chosen delay between 3.5 and 4.5 s, a gray block appeared on either the left- or right hand side of the screen, instructing subjects to initiate motor imagery of the respective hand. This block disappeared again after 6 s, indicating the end of the trial and start of the subsequent baseline period. In each session, 30 trials per condition were recorded in pseudo-randomized order. Each subject performed two sessions with a brief intermission in between, resulting in a total of 120 trials per subject. Prior to participation, each subject gave informed consent in accordance with guidelines set by the Max Planck Society.

2.2. Experimental data

During the experimental sessions, EEG was recorded at 121 electrodes (placed according to the extended 10-20 system) at a sampling rate of 500 Hz using a QuickAmp amplifier (BrainProducts GmbH, Gilching, Germany) with a built-in common-average reference. Electrode FzA was used as the ground electrode, and recordings were re-referenced to common average reference offline. Fourteen subjects (S1-S14) participated in this study, none of whom had known neurological disorders (five female, mean age 25.14

years with a standard deviation of 3.39 years, eleven right-handed). Four subjects had previously participated in studies involving motor imagery (S1, S2, S3, and S6). We aimed for impedances below $10\text{ k}\Omega$ at the start of the experiment. Electrodes exceeding this threshold, as well as those deemed to be noisy by visual inspection, were switched off by manually connecting them to the ground channel of the amplifier. None of the subjects participating in the present study participated in the study reported in [10].

2.3. Independent component analysis & artifact correction

In any non-invasive recording of the electromagnetic field of the brain, the activity of cortical sources may be obscured by artifactual components such as ocular- or muscular artifacts [12, 13]. To decrease the probability of data contamination by artifactual sources, we employed independent component analysis (ICA) to decompose the recorded EEG signals into (ideally) statistically independent components (ICs) [14, 15]. Specifically, the recorded data of each subject was first high-pass filtered using a 3rd order Butterworth filter with a cut-off frequency of 3 Hz, then reduced to 64 components by principal component analysis (PCA), and finally separated into ICs using the SOBI-algorithm [16]. ICs were rejected as artifactual if at least one of the following four criteria was met: (1) The spectrum did not show the $1/f$ -behaviour typical of cortical sources. In particular, sources that displayed a monotonic increase in spectral power starting around 20 Hz were rejected, as this is characteristic for muscular activity [13]. (2) Eye blinks were detectable in the time-series. (3) The topography did not show a dipolar pattern. (4) The time-series appeared to be contaminated by other noise sources such as 50 Hz line noise or large spikes. The time-series of the non-rejected ICs and their associated topographies were stored for subsequent analysis.

2.4. Decoding procedure

We adopted a standard decoding procedure in order to make our results applicable for a typical BCI-setup [17]. First, the non-rejected ICs were reprojected to the scalp. Then, a Laplacian filter was applied to the recorded data [18], and 18 channels, covering left- and right sensorimotor areas (C1, C3, C5, C3A, C5A, FC3, C3P, C5P, CP3, C2, C4, C6, C4A, C6A, FC4, C4P, C6P, CP4), were selected for further analysis. For each trial, log-bandpower was computed at every electrode in frequency bands of 2 Hz width, ranging from 7–15 Hz (the reason for the focus on the μ -rhythm is discussed in Section 4). Only the first 5.5 s of each motor-imagery phase were used for bandpower computation. This was carried out with a fast Fourier transform (FFT) in conjunction with a Hann window. The resulting ($18 \times 5 = 90$)-dimensional feature space was then used to train a linear ν -support vector machine (ν SVM) to discriminate trials of left- vs. trials of right-hand motor imagery [19]. In order to avoid overfitting, a 12-fold cross-validation procedure was employed. Parameter selection of the ν SVM was performed by 10-fold cross-validation on each of the 12 outer folds.

2.5. A trial-wise measure of BCI-performance

In order to measure BCI-performance on a trial-to-trial basis, the following metric was adopted [10]: For each subject, the scalar decision value of the ν SVM in the i^{th} trial was multiplied by the trial’s true class label $c_i \in \{-1, +1\}$. The resulting variable, subsequently denoted as the SMR quality score (SMRq), represents easy to classify trials by large positive values, uncertain trials by small values, and incorrectly classified trials by negative values. It thereby measures the capability of a subject to induce a lateralization of the SMR on a trial-to-trial basis, which facilitates an investigation of within-session variations in BCI-performance (cf. Figure 1, displaying the observed SMRq for Subject S1). We discuss the relation of the SMRq to average classification accuracy in Section 3.4.

2.6. Predicting trial-to-trial variations in BCI-performance

Prediction of the SMRq from bandpower in the γ -range was performed for each subject independently by linear regression. For each trial, log-bandpower in the high γ -range (70-80 Hz) was computed for every non-rejected IC, using only the last two seconds of each trial’s baseline, i.e., a time-window in which the subject did not know yet which type of motor-imagery to perform next. For the i^{th} trial, the ICs’ baseline power in the high γ -range is subsequently denoted by the vector $\boldsymbol{\gamma}_i$. The sequence $[\boldsymbol{\gamma}_1, \dots, \boldsymbol{\gamma}_{120}]$ was then low-pass filtered with a causal 3rd-order Butterworth filter with cut-off frequency 0.001 Hz. The rationale for this focus on very slow modulations of γ -power is discussed in Section 4. Finally, a linear regression model of the form

$$\text{SMRq}_i = \mathbf{a}^T \boldsymbol{\gamma}_i + b + \epsilon_i \quad (1)$$

with parameters $\{\mathbf{a}, b\}$ and i.i.d. noise $\epsilon \sim \mathcal{N}(0, \sigma_\epsilon)$ was learned by least-squares regression. The accuracy of this model was evaluated by computing Pearson’s correlation coefficient between measured and predicted SMRq with a 10-fold cross-validation procedure. Group-level prediction accuracy was evaluated by first standardizing the predicted/measured SMRq-values within each subject and then pooling across subjects.

2.7. Source localization

In order to identify which cortical areas predict BCI-performance, the regression weights in (1) were projected to the cortical level. First, the cortical origins of each IC used in (1) were localized using the BrainStorm toolbox [20]. A distributed source model with minimum-norm estimation was selected for this purpose, based on a standard head-model and standard electrode locations. The obtained cortical activation pattern of each IC was then weighted by its regression coefficient in (1) prior to averaging the patterns across all ICs associated with one individual subject. This resulted in one cortical map for each subject, displaying how γ -power at each cortical location enters into the prediction of the SMRq. These maps were then averaged across all subjects to obtain a grand-average plot.

3. Experimental Results

3.1. Decoding accuracy

The second column of Table 1 lists the classification results for distinguishing left- vs right-hand motor imagery. As is typical in BCI-studies on motor imagery, classification accuracies vary substantially, ranging from 50% to 95% with a mean of 70.1%. For $N = 120$ trials, an accuracy of 57.5% is required to reject the null-hypothesis of chance-level performance at significance level $\alpha = 0.05$ [21]. As such, the null-hypothesis could not be rejected for four of the 14 subjects (S7, S9, S11, and S14).

3.2. Trial-to-trial performance prediction

On the group-level, a correlation coefficient of $\rho_{\text{SMRq}} = +0.10$ was found between the measured and predicted SMRq (third column of Table 1). This is sufficient to reject the null-hypothesis of zero-correlation with $p \leq 0.0001$ ($N = 1680$, random permutation test with 10,000 iterations [22]), which provides strong support for the conclusion that γ -range oscillations can be used to predict BCI-performance on a trial-to-trial basis.

On the single-subject level, correlations ranged from $+0.42$ to -0.19 . Figure 2 displays the measured and predicted SMRq for subject S1 ($\rho_{\text{SMRq}} = +0.42$, left panel) and subject S11 ($\rho_{\text{SMRq}} = -0.17$, right panel). Slow drifts in performance in subject S1, i.e., on a time-scale of several minutes, are very well predicted by γ -power. Faster variations on a scale of several seconds, on the other hand, are not represented by the predicted SMRq. In subject S11, only variations in performance on a short time-scale are apparent, resulting in a poor prediction of the SMRq. In general, the SMRq could be predicted very well in subjects that exhibited performance variations predominantly on a time-scale of several minutes. Subjects in whom faster variations dominated did not show good prediction results. This is quantified in Figure 3, showing the measured SMRqs' spectra for subjects with positive and negative ρ_{SMRq} .

3.3. Source localization

Figure 4 displays the grand-average cortical map of regression weights used to predict BCI-performance (cf. Section 2.7). For better visualization, voxels with absolute activation smaller than 0.3 are displayed in gray. The map indicates that differences in γ -power between two fronto-parietal networks predict BCI-performance.

3.4. Relevance in terms of classification accuracy

In order to quantify the relevance of γ -power for BCIs in terms of average classification accuracy, Figure 5 displays group-average accuracy as a function of predicted SMRq. Here, all trials, that do not exceed a certain predicted SMRq, are discarded prior to computation of the classification accuracy. The resulting accuracy is relevant for the first

strategy outlined in Section 1, i.e., for rejecting trials that are unlikely to be correctly decoded.

By successively rejecting more and more trials, mean classification accuracy can be increased from 70.1% to 85%. While this is a substantial gain of +14.9%, it requires rejecting the majority of trials (92.9%). In practice, a sensible trade-off between enhanced accuracy and amount of rejected trials would have to be selected. It is noteworthy that classification performance decreases again if more than 92.9% of trials are rejected. This indicates that the linear model in (1) may not be adequate for predicting BCI-performance if extreme values of γ -power are observed.

4. Discussion

In this article, we have presented empirical evidence that differences in γ -power between two fronto-parietal networks can be used to predict BCI-performance on a trial-to-trial basis. This finding provides support for an eminent role of attentional networks in brain-computer interfacing: The positively-weighted areas in Figure 4 bear a close resemblance to the fronto-parietal network found to be activated during focused attention and working memory, while the negative weights are in good correspondence with cortical areas associated with the default-mode network [23-25]. Furthermore, resting-state activity in these networks is known to fluctuate at very low frequencies (< 0.1 Hz) [26, 27], which is consistent with the temporal variations in BCI-performance reported here (cf. Figure 3). We thus interpret our results as providing support for an influence of attentional networks on BCI-performance via modulation of the μ -rhythm.

As outlined in Section 1, there are multiple strategies by which our results might be used to enhance BCI performance. While we have demonstrated the feasibility of the first strategy, i.e., discarding trials that are unlikely to result in a correct inference of the subject's goal, significant gains in performance require a substantial reduction of the number of usable trials (cf. Figure 5). However, linear models may not be optimal for representing the relationship of γ -power and BCI-performance. It remains to be investigated whether more substantial gains can be achieved by non-linear models. Regarding the remaining strategies discussed in Section 1, the predictive power of γ -oscillations establishes attentional networks as potential causes of variations in BCI-performance [28, 29]. This is in agreement with our previous findings [10] and indicates that it may be feasible to use neurofeedback of fronto-parietal γ -power for teaching subjects how to induce a state-of-mind beneficial for operating a BCI. It remains to be established if subjects can learn how to volitionally modulate activity in these networks.

To conclude, we would like to emphasize that we have uncovered only a small aspect of BCI-performance variations. For instance, motor-imagery BCIs typically employ the μ - and the β -rhythm for decoding [30]. As these rhythms are likely to represent different neuronal processes [31], we have decided to solely focus on the μ -rhythm. Similar results to those reported here can also be obtained for β -rhythms, but are beyond the scope of this article. Furthermore, variations in BCI-performance take place on diverse time-

scales, ranging from several seconds to multiple minutes (cf. Figure 3). We found the power of fronto-parietal γ -oscillations to only predict those occurring on a time-scale of several minutes. In fact, we found the low-pass filtering of baseline γ -power across trials, as described in Section 2.6, a prerequisite for obtaining good predictions. Finally, the results reported here apply to healthy subjects only. As activity in the default-mode network has been found to be altered in patients diagnosed with amyotrophic lateral sclerosis (ALS) [32], we hope that our findings may also help to explain the current failure of patients in late stages of ALS to communicate via a BCI. Substantial work remains to be done to fully understand the neural determinants of good and bad BCI-performance in healthy subjects and patient populations.

References

- [1] P. Sykacek, S.J. Roberts, and M. Stokes. Adaptive BCI based on variational Bayesian Kalman filtering: an empirical evaluation. *IEEE Transactions on Biomedical Engineering*, 51(5):719–727, 2004.
- [2] C. Vidaurre, A. Schlogl, R. Cabeza, R. Scherer, and G. Pfurtscheller. A fully on-line adaptive BCI. *IEEE Transactions on Biomedical Engineering*, 53(6):1214–1219, 2006.
- [3] P. Shenoy, M. Krauledat, B. Blankertz, R.P.N. Rao, and K.R. Müller. Towards adaptive classification for BCI. *Journal of Neural Engineering*, 3:R13, 2006.
- [4] B. Varkuti, S. Halder, M. Bogdan, A. Kübler, W. Rosenstiel, R. Sitaram, and N. Birbaumer. SMR EEG-BCI aptitude in healthy subjects varies with the integrity of corpus callosum white matter. In G.R. Müller-Putz, R. Scherer, M. Billinger, A. Kreilinger, V. Kaiser, and C. Neuper, editors, *Proceedings of the 5th International BCI Conference 2011*, pages 104–107, 2011.
- [5] F. Nijboer, N. Birbaumer, and A. Kübler. The influence of psychological state and motivation on brain-computer interface performance in patients with amyotrophic lateral sclerosis – a longitudinal study. *Frontiers in Neuroscience*, 4, 2010.
- [6] Á. Barbero and M. Grosse-Wentrup. Biased feedback in brain-computer interfaces. *Journal of NeuroEngineering and Rehabilitation*, 7(34):1–4, 2010.
- [7] T.O. Zander and S. Jatzev. Towards context-aware BCIs: Exploring the information space of user, technical system and environment. *Journal of Neural Engineering*, 2011. in press.
- [8] E.M. Hammer, S. Halder, B. Blankertz, C. Sannelli, T. Dickhaus, S. Kleih, K.R. Müller, and A. Kübler. Psychological predictors of SMR-BCI performance. *Biological Psychology*, 2011. in press.
- [9] B. Blankertz, C. Sannelli, S. Halder, E.M. Hammer, A. Kübler, K.R. Müller, G. Curio, and T. Dickhaus. Neurophysiological predictor of SMR-based BCI performance. *NeuroImage*, 51(4):1303–1309, 2010.
- [10] M. Grosse-Wentrup, B. Schölkopf, and J. Hill. Causal influence of gamma rhythms on the sensorimotor rhythm. *NeuroImage*, 56(2):837–842, 2011.
- [11] M. Grosse-Wentrup. Fronto-parietal gamma-oscillations are a cause of performance variation in brain-computer interfacing. In *Neural Engineering (NER), 2011 5th International IEEE/EMBS Conference on*, pages 384–387. IEEE, 2011.
- [12] S. Yuval-Greenberg, O. Tomer, A.S. Keren, I. Nelken, and L.Y. Deouell. Transient induced gamma-band response in EEG as a manifestation of miniature saccades. *Neuron*, 58:429–441, 2008.
- [13] I.I. Goncharova, D.J. McFarland, T.M. Vaughan, and J.R. Wolpaw. EMG contamination of EEG: Spectral and topographical characteristics. *Clinical Neurophysiology*, 14:1580–1593, 2003.
- [14] T.P. Jung, S. Makeig, C. Humphries, T.W. Lee, M.J. McKeown, V. Iragui, and T.J. Sejnowski. Removing electroencephalographic artifacts by blind source separation. *Psychophysiology*, 37(2):163–178, 2000.

- [15] B.W. McMenamin, A.J. Shackman, J.S. Maxwell, D.R.W. Bachhuber, A.M. Koppenhaver, L.L. Greischar, and R.J. Davidson. Validation of ICA-based myogenic artifact correction for scalp and source-localized EEG. *NeuroImage*, 49:2416–2432, 2010.
- [16] A. Belouchrani, K. Abed-Meraim, J.-F. Cardoso, and E. Moulines. A blind source separation technique using second-order statistics. *IEEE Transactions on Signal Processing*, 45(2):434–444, 1997.
- [17] S.G. Mason, A. Bashashati, M. Fatourechhi, K.F. Navarro, and G.E. Birch. A comprehensive survey of brain interface technology designs. *Annals of Biomedical Engineering*, 35(2):137–169, 2007.
- [18] D.J. McFarland, L.M. McCane, S.V. David, and J.R. Wolpaw. Spatial filter selection for EEG-based communication. *Electroencephalography and Clinical Neurophysiology*, 103:386–394, 1997.
- [19] B. Schölkopf, A.J. Smola, R.C. Williamson, and P.L. Bartlett. New support vector algorithms. *Neural Computation*, 12:1207–1245, 2000.
- [20] J.C. Mosher, S. Baillet, F. Darvas, D. Pantazis, E.K. Yildirim, and R.M. Leahy. Brainstorm electromagnetic imaging software. In *5th International Symposium on Noninvasive Functional Source Imaging within the Human Brain and Heart (NFSI 2005)*, 2005.
- [21] G.R. Müller-Putz, R. Scherer, C. Brunner, R. Leeb, and G. Pfurtscheller. Better than random? A closer look on BCI results. *International Journal of Bioelectromagnetism*, 10(1):52–55, 2008.
- [22] D.S. Moore and G.P. McCabe. *Introduction to the Practice of Statistics*. WH Freeman & Co, 2005.
- [23] M.D. Fox, A.Z. Snyder, J.L. Vincent, M. Corbetta, D.C. Van Essen, and M.E. Raichle. The human brain is intrinsically organized into dynamic, anticorrelated functional networks. *Proceedings of the National Academy of Sciences*, 102(27):9673–9678, 2005.
- [24] M.D. Greicius, B. Krasnow, A.L. Reiss, and V. Menon. Functional connectivity in the resting brain: a network analysis of the default mode hypothesis. *Proceedings of the National Academy of Sciences*, 100(1):253, 2003.
- [25] M.E. Raichle, A.M. MacLeod, A.Z. Snyder, W.J. Powers, D.A. Gusnard, and G.K. Shulman. A default mode of brain function. *Proceedings of the National Academy of Sciences*, 98(2):676–682, 2001.
- [26] M. Corbetta, G. Patel, and G.L. Shulman. The reorienting system of the human brain: from environment to theory of mind. *Neuron*, 58(3):306–324, 2008.
- [27] A.L. Ko, F. Darvas, A. Poliakov, J. Ojemann, and L.B. Sorensen. Quasi-periodic fluctuations in default mode network electrophysiology. *The Journal of Neuroscience*, 31(32):11728, 2011.
- [28] C.W.J. Granger. Investigating causal relations by econometric models and cross-spectral methods. *Econometrica: Journal of the Econometric Society*, 37(3):424–438, 1969.
- [29] Judea Pearl. *Causality: Models, Reasoning, and Inference*. Cambridge University Press, 2000.
- [30] G. Pfurtscheller and C. Neuper. Motor imagery and direct brain-computer communication. *Proceedings of the IEEE*, 89(7):1123–1134, 2001.
- [31] N.E. Crone, D.L. Miglioretti, B. Gordon, J.M. Sieracki, M.T. Wilson, S. Uematsu, and R.P. Lesser. Functional mapping of human sensorimotor cortex with electrocorticographic spectral analysis. I. alpha and beta event-related desynchronization. *Brain*, 121(12):2271, 1998.
- [32] B. Mohammadi, K. Kollwe, A. Samii, K. Krampfl, R. Dengler, and T.F. Münte. Changes of resting state brain networks in amyotrophic lateral sclerosis. *Experimental neurology*, 217(1):147–153, 2009.

5. Tables & Figures

Table 1. Decoding accuracy (second column) and correlation coefficient between measured and predicted SMRq (third column).

Subject	P_a [%]	ρ_{SMRq}
S1	83.3	+0.42
S2	95.0	+0.41
S3	85.8	-0.12
S4	80.0	+0.10
S5	66.7	+0.08
S6	70.0	+0.18
S7	52.5	+0.14
S8	64.2	+0.16
S9	52.5	+0.09
S10	82.5	+0.11
S11	55.8	-0.17
S12	69.2	-0.19
S13	73.3	+0.06
S14	50.0	+0.04
Group	70.1	+0.10

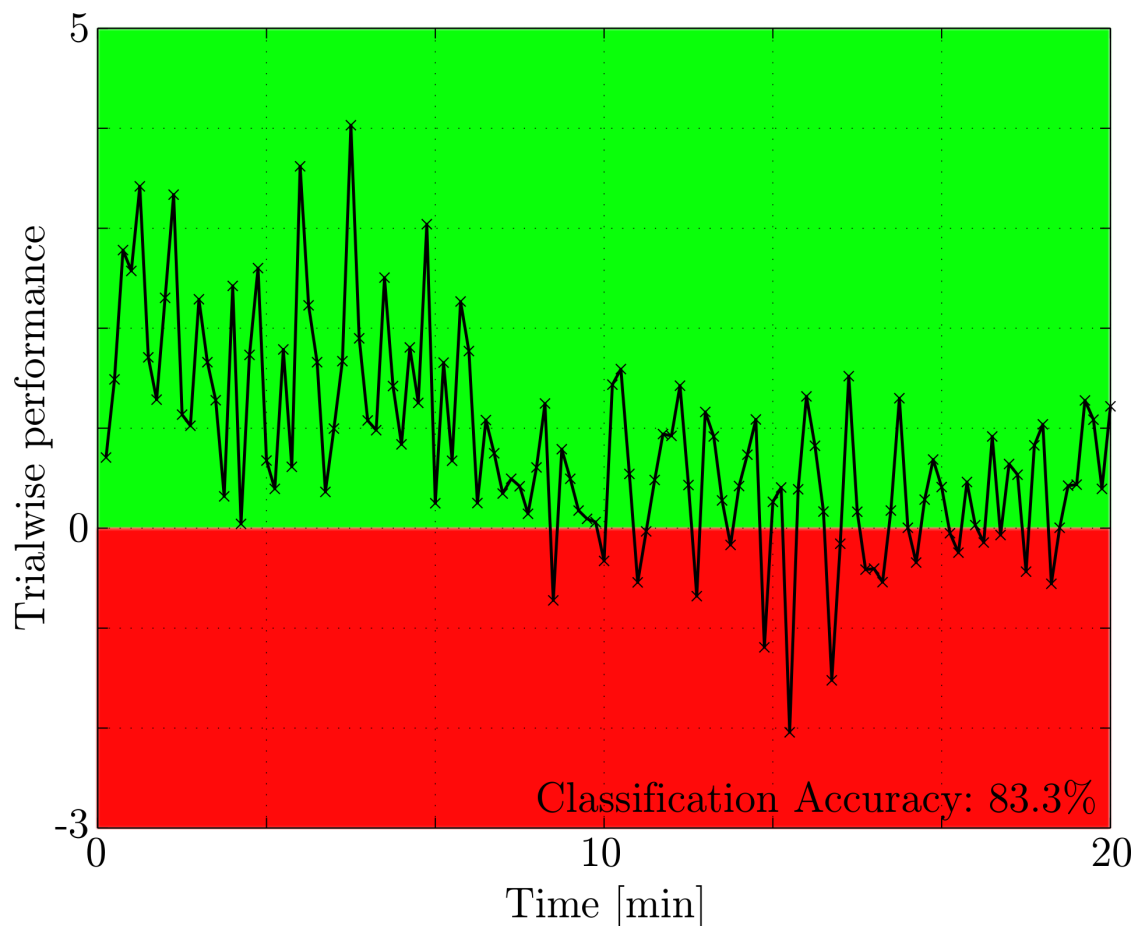


Figure 1. Trial-to-trial variations in BCI-performance of one representative subject over the course of one experimental session. See text for details.

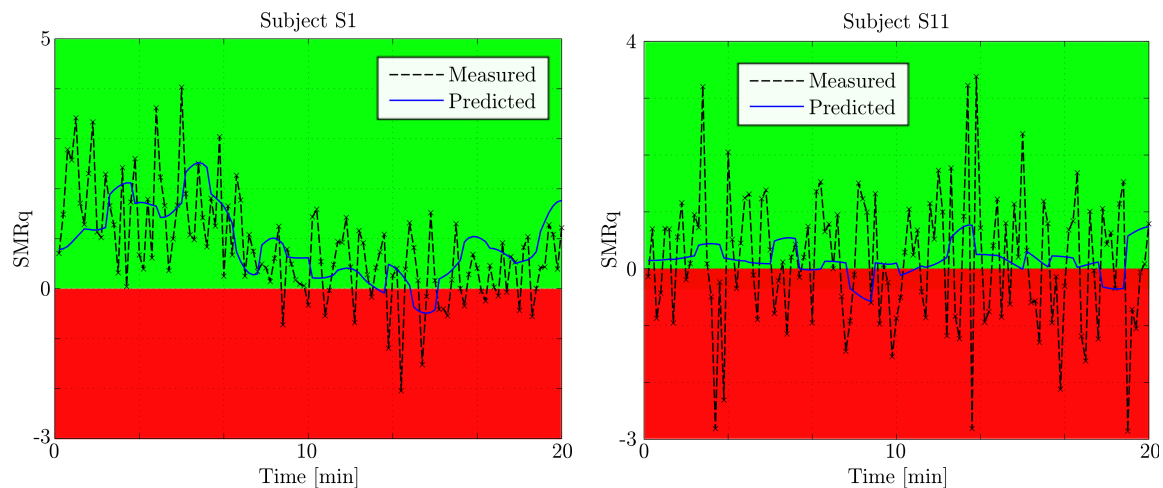


Figure 2. Measured and predicted SMRq for subject S1 (left panel) and subject S11 (right panel). Note that the predicted SMRq explains variations in BCI-performance on a time scale of several minutes (as predominantly seen in subject S1), but fails to account for variations on the order of seconds (that dominate in subject S11).

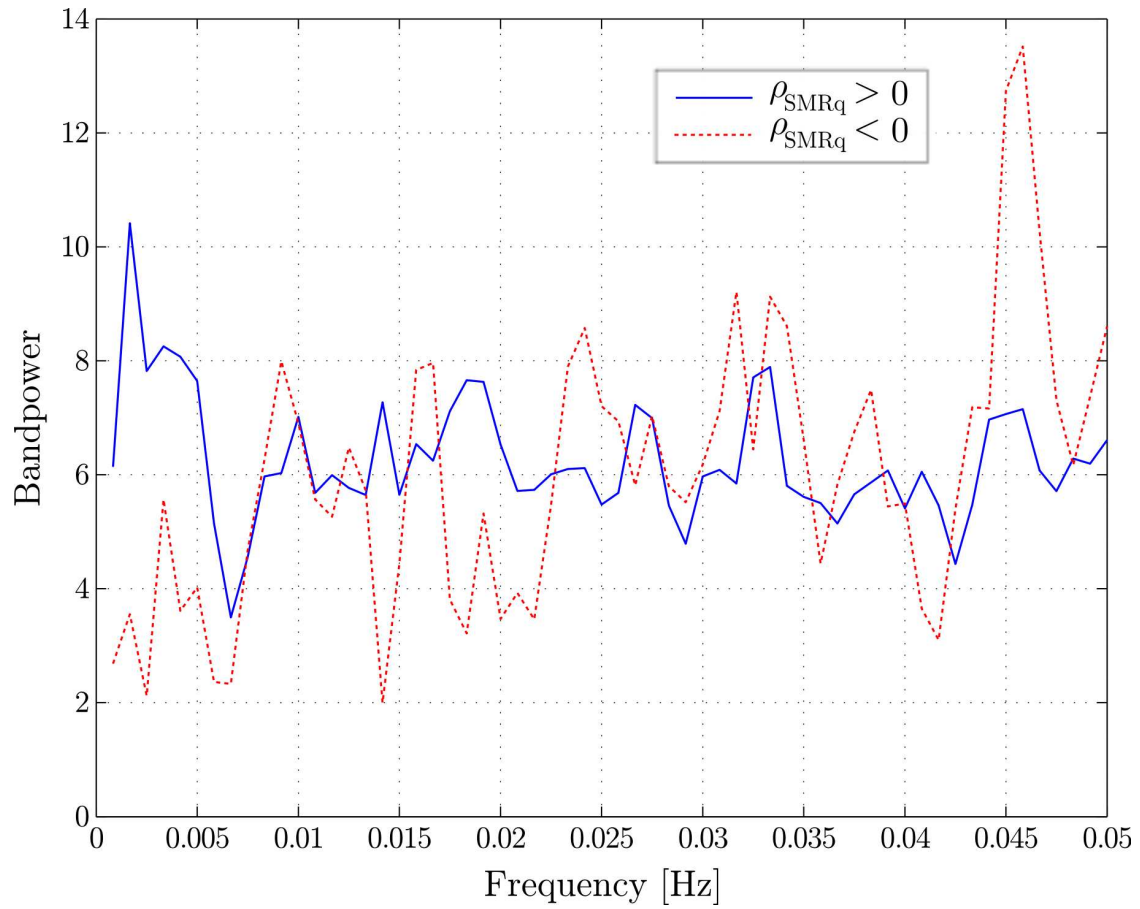


Figure 3. Spectra of measured SMRq averaged across subjects with $\rho_{\text{SMRq}} > 0$ and $\rho_{\text{SMRq}} < 0$. The former group displays a peak at 0.002 Hz, while the SMRq of the latter group is dominated by a peak at 0.046 Hz.

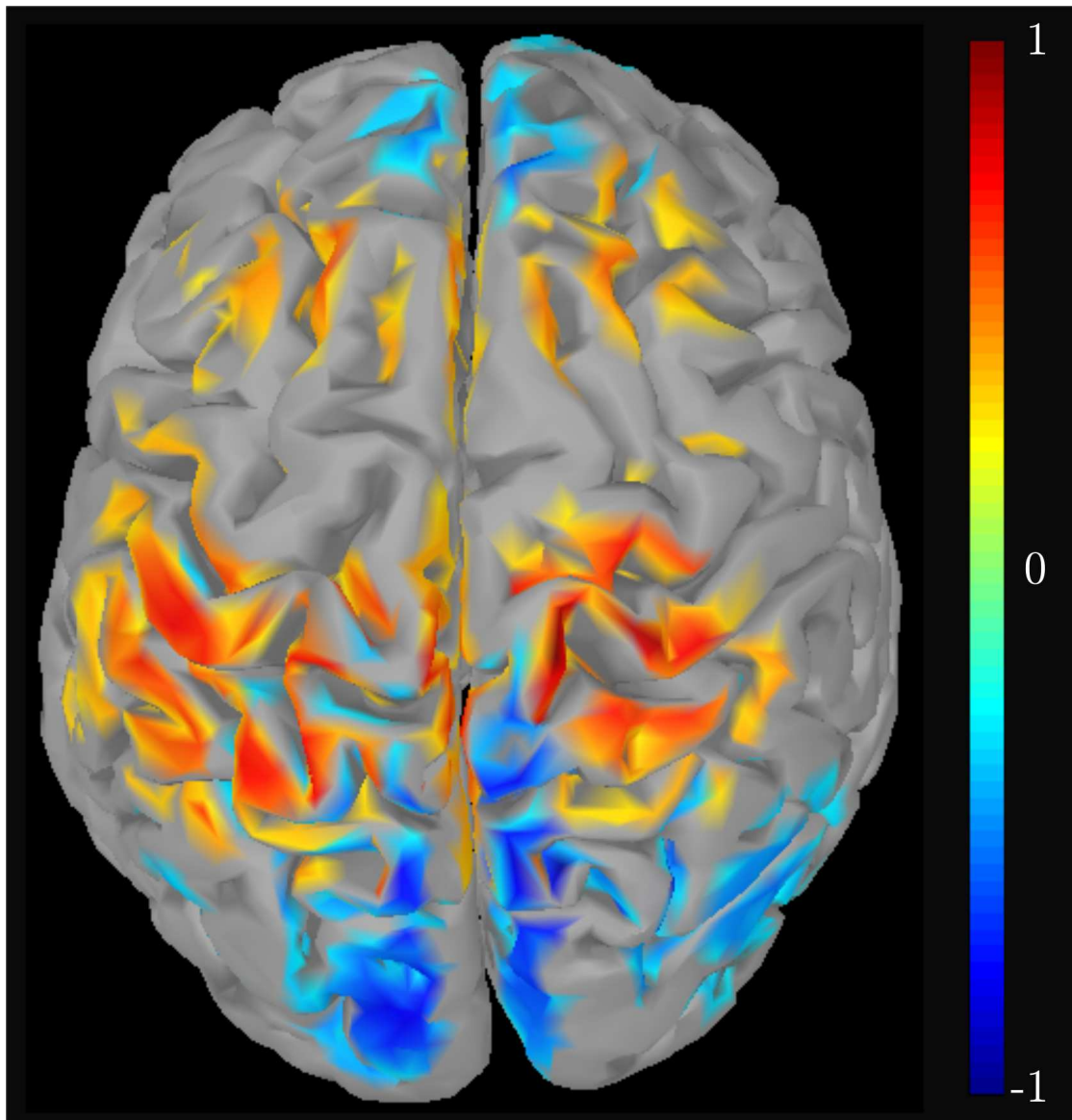


Figure 4. Grand-average cortical map of regression weights used to predict BCI-performance (normalized units and thresholded at 30%). Performance is predicted from differences in γ -power between two fronto-parietal networks. See Section 2.7 for details.

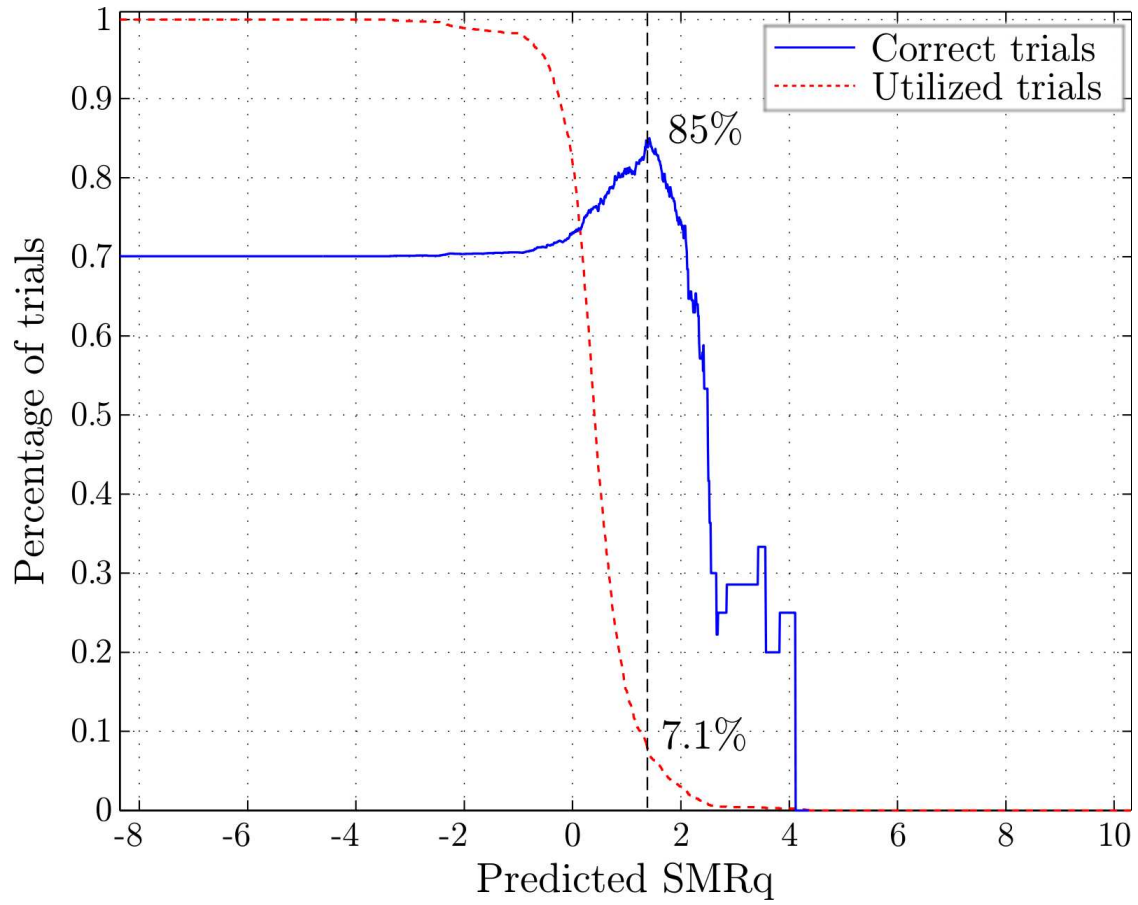


Figure 5. Group-average classification accuracy as a function of minimum predicted SMRq.